JOURNAL OF GEOPHYSICAL RESEARCH, VOL. 98, NO. A11, PAGES 18,879–18,893, NOVEMBER 1, 1993

Recent Solar Extreme Ultraviolet Irradiance Observations and Modeling: A Review

W. KENT TOBISKA

TELOS/Jet Propulsion Laboratory, Pasadena, California

For more than 90 years, solar extreme ultraviolet (EUV) irradiance modeling has progressed from empirical blackbody radiation formulations, through fudge factors, to typically measured irradiances and reference spectra as well as time-dependent empirical models representing continua and line emissions. A summary of recent EUV measurements by five rockets and three satellites during the 1980s is presented along with the major modeling efforts. The most significant reference spectra are reviewed and three independently derived empirical models are described. These include Hinteregger's 1981 SERF1, Nusinov's 1984 two-component, and Tobiska's 1990/1991 SERF2/EUV91 flux models. They each provide daily full-disk broad spectrum flux values from 2 to 105 nm at 1 AU. All the models depend to one degree or another on the long time series of the Atmosphere Explorer E (AE-E) EUV database. Each model uses ground- and/or space-based proxies to create emissions from solar atmospheric regions. Future challenges in EUV modeling are summarized including the basic requirements of models, the task of incorporating new observations and theory into the models, the task of comparing models with solar-terrestrial data sets, and long-term goals and modeling objectives. By the late 1990s, empirical models will potentially be improved through the use of proposed solar EUV irradiance measurements and images at selected wavelengths that will greatly enhance modeling and predictive capabilities.

INTRODUCTION

The requirement for an accurate estimate of the solar extreme ultraviolet (EUV) flux, a fundamental thermospheric energy input, is driven by the effort to provide a self-consistent model of the ionospheric and neutral atmospheric compositional and temperature structure that compares favorably with in situ and remotely sensed measurements. Research to understand the energy balance in the thermosphere has produced considerable activity over the past three decades to measure and model the solar EUV irradiance variations.

The broad spectrum of solar EUV irradiances at wavelengths below 105 nm has not been continuously measured since the Atmosphere Explorer E (AE-E) mission which ceased EUV observations in December 1980. The one exception has been the recent San Marco solar EUV experiment from March to December 1988. These measurements are just completing the calibration process. Short-duration rocket observations have been made on five occasions during the 1980s and these data sets serve as useful absolute reference points but do not contribute information about the long-term variations.

Given the paucity of continuously measured EUV data, a state of affairs termed the "EUV hole" by *Donnelly* [1987*a*] and graphically shown in Figure 1, three independently derived empirical solar EUV models have been developed which estimate the daily average full-disk flux variation for up to 39 wavelength groups or discrete lines at 1 AU. The model of *Hinteregger et al.* [1981] which was designated SERF1 by the World Ionosphere - Thermosphere Study (WITS) program called the Solar Electromagnetic Radiation Flux Study (SERFS), the *Nusinov* [1984] two-component model, and the EUV91 model [*Tobiska*, 1991], which evolved out of the SERFS program [*Donnelly*, 1988*a*] all utilize the AE-E EUV data set as either the only time-varying input to the model (SERF1 and Nusinov) or as a significant component of the model (EUV91). All of the empirical solar EUV models are similarly limited to producing only full-disk emissions with daily average values often with a relatively coarse wavelength scale. The complexity in the models has increased with their attempt to reproduce solar rotational irradiance variations and other temporal phenomena. Additional complications have been introduced as the models attempt to reproduce emissions from specific solar temperature regions and from the evolution of disk features. Distinct periods in empirical solar EUV modeling are summarized by *Simon and Tobiska* [1991] including early theoretical description, data collection, and empirical modeling.

Paper number 93JA01943.
0148-0227/93/93JA-01943$05.00

BACKGROUND

Early Theoretical Description (1900-1937)

The first empirically modeled, time-independent, solar EUV irradiance was described on October 19, 1900, at a meeting of the Berlin Physical Society. Planck, who had been searching for a way to reconcile the Wien and Rayleigh-Jeans formulations of the spectral distribution of blackbody radiation, revealed to the gathering an empirical formulation that fit quite well the experimental data of the day [*Planck*, 1901]. This function, Planck's law, is shown in Figure 2 compared with the Rayleigh-Jeans and Wien's energy densities and demonstrates the well-known equation

$$U(\lambda) = \frac{8\pi hc\,\lambda^{-5}}{e^{hc/\lambda kT} - 1} \quad . \tag{1}$$

This formulation, which assumed that the energy of an oscillator can only take on discrete values, set the stage for the quantum theory of light and solved the "ultraviolet catastrophe." This expressive term referred to the infinitely increasing UV energy with shorter wavelengths in the Rayleigh-Jeans formulation seen in Figure 2.

For several decades it was expected that the solar irradiance in the EUV followed the Planck blackbody spectrum. Finally, *Saha* [1937] noted that the only reasonable explanation for the forma-

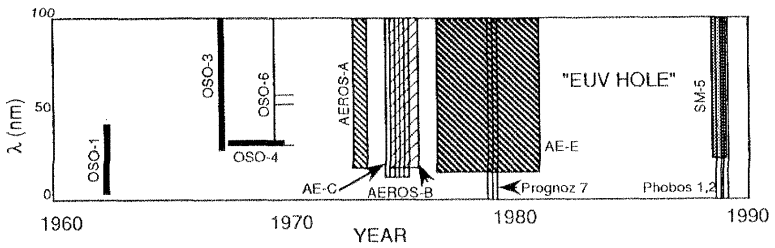

Fig. 1. Time and wavelength coverage of EUV measurements from satellites (adapted from *Schmidtke* [1992]).

tion of the first negative bands of nitrogen in the night sky observed at high-altitude sunrise and sunset ($z > 200$ km) was ionization from solar EUV ($0.1 < 66$ nm). His contribution to the field of empirical EUV modeling was based on estimating a photon flux value. He noted that the number of photons available for N_2 ionization, according to Planck's law, was insufficient given the total ion production rate needed to maintain a total ionization of 3×10^{10} electrons [*Chapman*, 1931]. Even if only 10% of the ionization were due to N_2, Saha concluded that an "ultraviolet excess factor" of 1×10^6 more photons would be needed to maintain the ionization compared to the theoretical flux provided by a solar blackbody at 6500 K. Thus a "fudge factor" of a million times more photons in the EUV than those predicted by Planck's law became the next de facto EUV model.

Data Collection (1946-1980)

It was not until successful sounding rocket flights were made above the atmosphere that solar EUV observations were actually taken. The first solar UV flux from a sounding rocket was obtained shortly after the Second World War [*Baum et al.*, 1946]. These rocket experiments later led to the first EUV photographic spectra below 100 nm which were obtained through photographs sensitive in the FUV and later EUV. The early history is presented in a summary by *Tousey* [1961]. The first spectrophotometric solar EUV measurements down to 6 nm were presented by *Hinteregger* [1960] and the broad spectrum between 30 and 120 nm was described by *Hall et al.* [1963]. These observations were followed by rocket flights and satellite measurements that filled in spectral gaps or provided information leading to the revision of the earlier results. *Timothy* [1977] reviewed the history of observations from 30 to 120 nm through the mid-1970s.

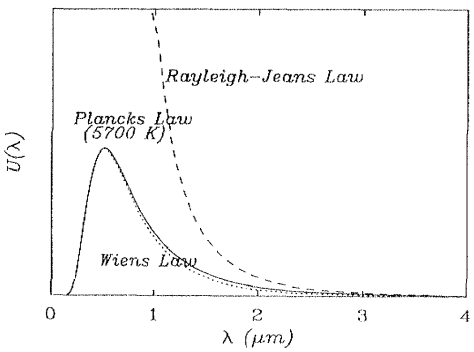

Fig. 2. Comparison of blackbody radiation for Planck's law, Wien's law, and Rayleigh-Jeans law. The Planck energy density spectrum fit experimental data of the day. Relative units of $U(\lambda)$ are in energy density. This spectral distribution is for a 5700 K blackbody (e.g., the Sun).

Figure 3 shows the solar spectrum published by *White* [1977] as a compilation of these early observations. The wealth of emission lines in the EUV, compared to the Planck solar blackbody in Figure 2, testifies to the remarkable observational progress in the three decades following World War II. Later, *Schmidtke* [1984], *Lean* [1987], *Rottman* [1988], and *Tobiska* [1991] summarized EUV observations from 10 to 120 nm through the mid-1980s. *Feng et al.* [1989] have provided a useful intercomparison of the integrated flux from 2 to 10 nm and 5 to 57.5 nm for many of the rocket observations of the 1970s and 1980s. *Schmidtke* [1992] has tabulated the observation periods, wavelength ranges, and results of the satellite missions monitoring the EUV during this same period.

Data Collection (1981-1989)

There are five rocket and three satellite data sets of the measured solar EUV irradiance that were obtained during the decade of the 1980s following the AE-E mission. In general, the rocket-measured irradiances have provided more accuracy in the measurements of the absolute solar flux below 57.5 nm and have provided calibration opportunities for one satellite data set which is just completing it's calibration analysis.

The University of Southern California (USC) has flown three rocket experiments in 1982, 1983, and 1988. *Carlson et al.* [1984], *Ogawa and Judge* [1986], and *Ogawa et al.* [1990] describe these flights in detail. In brief, the August 10, 1982 flight occurred during high solar activity conditions where the 10.7-cm radio flux, $F_{10.7}$, was 210×10^{-22} W m^{-2} Hz^{-1}. The instrument consisted of a windowless rare-gas (neon) ionization chamber to measure the total absolute EUV irradiance between 5 and 57.5 nm to $\pm$ 7% uncertainty. The same instrument was reflown a year later on August 16, 1983, when the $F_{10.7}$ was 132 representing moderate to low solar activity conditions. The USC group flew a third rocket experiment on October 24, 1988, using a newly developed silicon photodiode to obtain the integrated absolute solar irradiance between 5 and 80 nm with an uncertainty of $\pm$14%. The $F_{10.7}$ of 168 on this date represented moderate solar activity.

The University of Colorado flew two rockets in 1988 [*Woods and Rottman*, 1990] and 1989 [*Woods and Rottman*, 1990; T. N. Woods, private communication, 1991] which measured solar EUV irradiance. The first, launched on November 10, 1988, included an EUV spectrograph that measured irradiances between 30 and 114 nm with an average wavelength-dependent uncertainty of $\pm$ 13% and spectral resolution of 0.5 to 1 nm. The $F_{10.7}$ of 148 on this date represented moderate solar activity and this experiment has been used to calibrate the San Marco satellite EUV measurements discussed below. The second flight on June 20, 1989 used the same instrument when $F_{10.7}$ was 243 which represented high solar activity.

The San Marco 5 satellite carried the Airglow Solar Spectrometer Instrument (ASSI) during its mission between March and

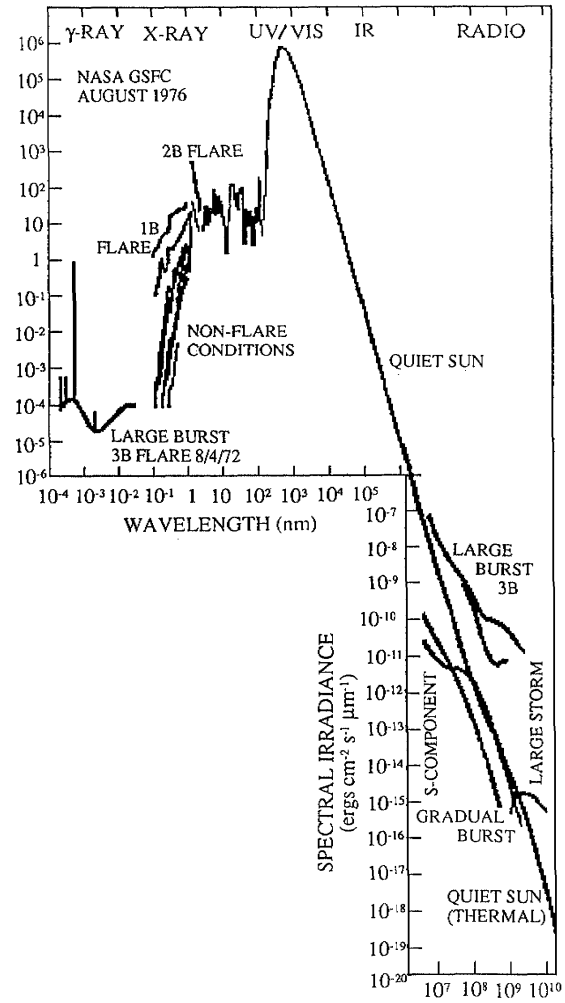

Fig. 3. The solar spectrum from gamma rays to radio wavelengths from *White* [1977].

December 1988. *Schmidtke et al.* [1985], *Schmidtke et al.* [1992], and *Schmidtke et al.* [1993] describe the instrument and preliminary results. The instrument consisted of two spectrometers covering the wavelength region of 28 nm to the visible with a resolution of approximately 1 nm. Preliminary conclusions (T. N. Woods, private communication, 1992) indicate that the contrast ratios for both chromospheric and coronal emissions measured by ASSI are similar to those derived using AE-E data, while daily deviations from simple empirical relationships are of the order of 30%.

The Prognoz 7 satellite operated between November 1978 and February 1979 during high solar activity. It measured solar EUV irradiances with an instrument developed by the Institute of Applied Geophysics of the State Committee for Hydrometeorology using a thermoluminescent phosphorus $CaSO_4$ (Mn) detector [*Kazachevskaya et al.*, 1985]. This instrument was sensitive to the integrated wavelength region of 1 to 130 nm; daily variability consistent with solar rotational effects has been described by *Ivanov-Kholodny and Kazachevskaya* [1981] and *Kazachevskaya and Lomovsky* [1992].

The Phobos 1 and 2 spacecraft en route to Mars (July to August 1988 and July 1988 to March 1989, respectively) carried the Solar Ultraviolet Radiometer (SUFR) instruments that measured solar EUV irradiances on a daily basis and was particularly sensitive to solar flares at integrated wavelengths less than 130 nm. *Kazachevskaya et al.* [1991] and *Kazachevskaya and Lomovsky* [1992] describe the preliminary results of those observations during large M and X class flares.

MODELING

EUV Irradiance Modeling (Reference Spectra 1965-1992)

The first comprehensive review of solar EUV modeling was conducted by *Schmidtke* [1984] and covered the period through the early 1980s. A brief synopsis of the activities of this period is given here. Following a successful rocket observation of a broad EUV spectrum in 1963, *Hinteregger et al.* [1965] tabulated an EUV flux standard spectrum for quiet solar conditions. The early results were later revised and corrected, leading to a spectrum of "medium" solar activity with nonflaring conditions [*Hinteregger*, 1970]. This was followed by the *Donnelly and Pope* [1973] compilation of an EUV model spectrum for moderate solar activity that summarized numerous successful rocket and satellite observations up to the early 1970s. Figure 4 shows the Donnelly and Pope spectrum where moderate solar activity was defined when $F_{10.7}$ was 150. *Hinteregger* [1976] reviewed the advances in measuring EUV irradiances following the Atmospheric Explorer C (AE-C) mission in the mid-1970s while *Heroux and Hinteregger* [1978] released a revised reference spectrum for moderate solar activity based upon the detailed study of a 1974 rocket flight. *Roble and Schmidtke* [1979] contributed a description of a variety of typical EUV flux cases for different solar conditions applied to aeronomical calculations. The most recent reference spectrum [*Schmidtke et al.*, 1992] has been provided through the San Marco ASSI calibration based upon the *Woods and Rottman* [1990] sounding rocket data. Figure 5 shows this spectrum for moderate solar activity ($F_{10.7} \approx 150$) in 1-nm intervals.

Figure 5 shows that although there is general agreement in the overall magnitude of important emission features, there are also differences in the ASSI spectrum compared with SERF1. For example, the ASSI emission lines of Lyman-α (121.6 nm), Lyman-β

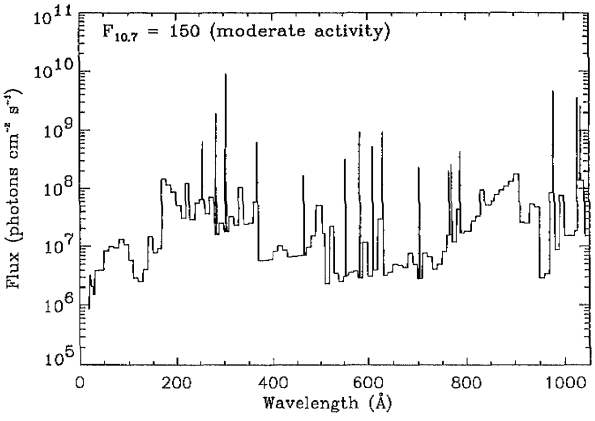

Fig. 4. Moderate solar activity spectrum compiled from several rocket observations [*Donnelly and Pope*, 1973]. Several discrete lines that are the most significant EUV emission lines in terms of magnitude are shown. The remaining flux (both lines and intervals) from Table 2 in Donnelly and Pope has been binned in 1-nm bins except for emissions below 3.1 nm where the average bin size is 0.3 nm. The abscissa wavelength conversion is 1 Å = 0.1 nm.

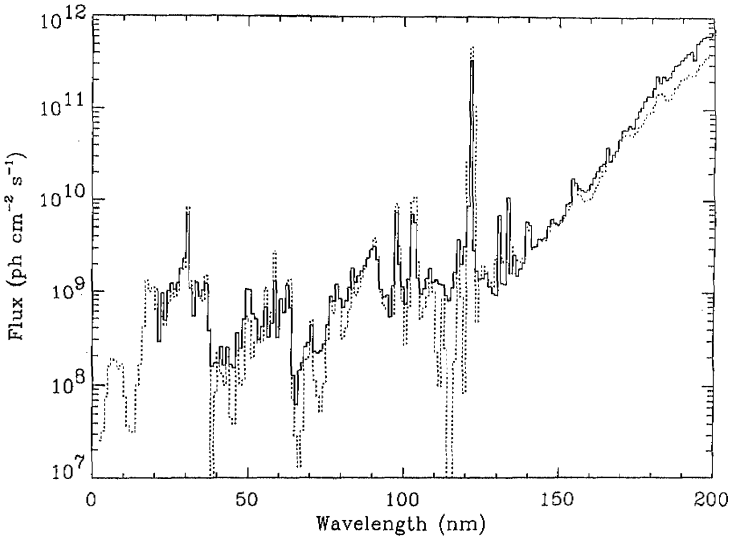

Fig. 5. ASSI solar EUV and FUV irradiance spectrum in 1 nm intervals (solid line) compared with modeled EUV flux from SERF1 (dashed line). The figure is from *Schmidtke et al.* [1992].

(102.6 nm), C III (97.7 nm), He I (58.4 nm), and He II (30.4 nm) all have smaller magnitude than SERF1. The He I and H Lyman continua have different slopes compared with each other. This suggests that the reference spectra and models still require a closer correspondence with one another.

As noted by *Simon and Tobiska* [1991], this period of EUV modeling was characterized by the presentation of reference spectra under a variety of solar conditions, by the categorizing of quiet, moderate, and active solar condition spectra, and by the description of the primary line and continua emission features. Important morphological features of the irradiance time series from satellite observations were described by *Timothy* [1977] including the 27-day variation corresponding to solar rotational effects with a peak-to-valley ratio of ± 15% for emissions originating in the solar chromosphere and the hint of active region evolution on longer time scales. *Rottman* [1988] noted that the EUV irradiances varied with the 11-year solar cycle and had a maximum-to-minimum ratio ranging from a factor of 2 to greater than 10 depending upon the solar source region for the wavelength.

By the end of the 1970s, it had become customary to represent solar EUV flux with the $F_{10.7}$ values [*Neupert*, 1967; *Hall and Hinteregger*, 1970; *Chapman and Neupert*, 1974; *Schmidtke*, 1976], although it has been pointed out [*Timothy*, 1977; *Donnelly*, 1982; *Donnelly et al.*, 1986*a*] that the $F_{10.7}$ is an unreliable indicator of EUV irradiance variability. *Hedin* [1984], *Donnelly et al.* [1986*b*], *Donnelly* [1987*b*], *Tobiska* [1988, 1990], *Tobiska and Barth* [1990], and *Donnelly and Puga* [1990] additionally describe the correlations of full-disk EUV irradiances with $F_{10.7}$. *Neupert* [1992] describes in detail the correlations between specific solar EUV emission lines and the solar 10.7- and 21-cm measurements in one spatial dimension.

Despite the tremendous observational advances of the period, the primary weaknesses that existed in solar EUV modeling could be attributed to the lack of long-term daily irradiance measurements combined with limited proxy representation of the flux. Reference spectra represented general levels of solar activity and provided more spectral detail than had been previously available.

EUV Irradiance Proxies

Prior to a continued discussion of EUV irradiance modeling, and particularly related to the effort to improve proxy representation of EUV flux, it is useful to describe those proxies, or indices, which have been correlated to various EUV emissions. Just as modeling has evolved over time, so has the use of proxies in order to estimate the EUV irradiances.

The most common proxy of solar EUV irradiance is the $F_{10.7}$ which was previously called the Covington index. The 27-day variability in this solar radiometric emission, coincident with the appearance of sunspots, was first described from ground-based daily measurement during the late 1940s [*Covington*, 1948]. The daily $F_{10.7}$, formerly measured regularly at the Algonquin Observatory in Ottawa since February 1947, is now measured with automated equipment at the Penticton (British Columbia) observatory since June 1991. *Gelfreikh* [1992] reviews the observational methods of solar radio astronomy and includes the main mechanisms for radio radiation generation. *Tapping* [1987] describes the two primary emission components of bright, compact sources and weaker, diffuse emission of the $F_{10.7}$.

The early connections of $F_{10.7}$ with the EUV irradiances were made through a sequence of events. *Roemer et al.* [1983] summarize some of the early connections between the solar EUV, the decimetric indices, and the thermospheric density variations. First, observations of 27-day variations in satellite drag [*Jacchia*, 1958] were linked to solar rotational radiation variation in $F_{10.7}$. This 1958 article referred to a previous suggestion that the thermospheric densities actually varied, although it was known at the time that $F_{10.7}$ did not contribute to heating, ionization, nor dissociation processes in the atmosphere. Much more energetic radiation in the UV and EUV was needed to accomplish those tasks. The first conclusive evidence of solar EUV irradiance (He I 30.4 nm, Fe XV 28.4 nm, and Fe XVI 33.5 nm) variation with a 27-day periodicity corresponding to the $F_{10.7}$ and sunspot solar rotational variability was obtained by the OSO 1 satellite [*Neupert et al.*, 1964].

crete lines could be modeled with time variation. An empirically determined function that fit the $F_{10.7}$ background provided a new capability for predicting this background component. Figure 7 shows the Nusinov $F_{10.7}$ background component (chromospheric network), and (4) describes his irradiance model as

$$I_\lambda = B_0 + B_1 (F_b - A)^{2/3} + B_2 (F_{10.7} - F_b)^{2/3} \quad (4)$$

where the first term is the background component, the second term is the active region component, and the A, B_0, B_1, and B_2 coefficients are found in the work by *Nusinov* [1984].

The Nusinov background component is

$$F_b = 63 + 482 \sin^{3.7}(\pi t/T)\, e^{-5.2t/T} \quad (5)$$

where t is time in years from the beginning of the cycle and T is the period of the cycle also in years. *Bruevich and Nusinov* [1984] extended this model throughout the EUV from 10 to 105 nm and *Nusinov* [1992] extended the model between 1 and 10 nm in addition to providing a method for determining the F_b background component for cycles 20 and 21.

The third independent modeling effort by *Tobiska* [1988] was characterized by the development of a two-index EUV flux model based on the *Hinteregger et al.* [1981] class model concept and the AE-E data set. It used the H Lyman-α to estimate the chromospheric irradiances and 0.1 to 0.8 nm X rays to estimate the coronal irradiances. *Tobiska and Barth* [1990] changed and improved this model by replacing the 0.1 to 0.8 nm X ray index with the $F_{10.7}$ daily values for use in estimating coronal EUV fluxes and by incorporating additional rocket EUV measurements to lower the uncertainty of the absolute irradiance values. This fourth empirical model by Tobiska and Barth was subsequently designated SERF2 [R.F. Donnelly, private communication, 1989; *Tobiska and Barth*, 1990] and covered the time frame between October 1981 and April 1989. *Tobiska* [1990] detailed the SERF2 model development.

SERF1 and SERF2 were compared by *Lean* [1990] over timescales of the 27-day solar rotation and the 11-year solar cycle. Significant differences were found between the models and between each model and the data sets upon which they were based. The differences appeared in the estimation of absolute intensities, the magnitude of peak-to-valley variation of irradiance due to solar rotation, and the maximum-to-minimum flux values over the 11-year solar cycle. Lean concluded that neither the models nor measurements yet provided a consistent picture of long-term variability in the EUV portion of the Sun's spectrum.

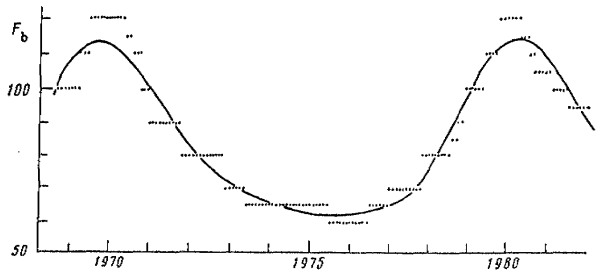

Fig. 7. *Nusinov* [1984] provided a $F_{10.7}$ background emission which is representative of the chromospheric network. He determined an empirical fit to the data given in (5) in the text. The units of F_b are 1×10^{-22} W m^{-2}Hz^{-1}. The abscissa value is time labeled with years.

In an effort to address the weaknesses of SERF2 and in order to assist the evaluation of the solar data from the San Marco Airglow Solar Spectrometer Instrument (ASSI) [*Tobiska et al.*, 1993], the SERF2 model was substantially revised [*Tobiska*, 1991]. This fifth model, called EUV91, represents an advance over the previous EUV models in proxy use, modeling technique, consistency of model results with data sets, and ability to incorporate into the model new solar data sets and recent proxy measurements. The model extends from 1947 to the present for coronal EUV full-disk irradiances and from 1976 to the present for chromospheric EUV full-disk irradiances. The solar Lyman-α (121.6 nm) emission line and He I 1083-nm EW measurements are used as the independent model parameters for the chromospheric irradiances while the $F_{10.7}$ daily and 81-day running mean values are the independent parameters for the coronal and transition region irradiances. The results of the model are full-disk photon fluxes at 1 AU for 39 EUV wavelength groups and discrete lines between 1.8 and 105 nm for a given date. Data from the OSO1/3/4/6, AEROS A, AE-E satellites and six rocket data sets are used in the model development. The irradiances from this model are given as

$$F(\lambda,t) = a_0(\lambda) + \sum_{i=1}^{4} a_i(\lambda) F_i(t) \quad (6)$$

where $F_i(t)$ are the proxy data sets. For example, $F_1(t)$ is Lyman-α, $F_2(t)$ is He I 1083-nm EW scaled to Lyman-α values, $F_3(t)$ is daily $F_{10.7}$, and $F_4(t)$ is the 81-day running mean value of $F_{10.7}$. The $a_i(\lambda)$ coefficients are tabulated by *Tobiska* [1991]. Missing proxy data are substituted through an empirical relationship with another proxy for which data exist on given dates. Figure 8 shows three examples of this model under low, moderate, and high solar activity conditions on the same wavelength scale as SC#21REFW. As a detailed example, Table 1 lists the EUV91 irradiance values for the moderate solar activity case on November 10, 1988, i.e., the date of the LASP rocket [*Woods and Rottman*, 1990]. Figure 9, adapted from *Ogawa et al.* [1990], shows a comparison of the model with several rocket flights and two previous models, i.e., those of *Donnelly and Pope* [1973] and SC#21REFW [*Hinteregger et al.*, 1981], for the 5 to 57.5 nm integrated flux.

A sixth model, SERF3, is presently under development as a full-disk multiple proxy model for chromospheric and coronal emissions. It correlates Mg II (c/w), Ca K 0.1 nm index, He I 1083-nm EW, $F_{10.7}$, 530.3-nm, and 0.1- to 0.8-nm data with the AE-E data set (R. F. Donnelly, private communication, 1993).

The SERF program concluded with the end of WITS on December 31, 1989. Since then, much of the international collaborative effort to study long-term changes in the solar total and spectral irradiance has been centered in the Solar Electromagnetic Radiation Study 22 (SOLERS22). The SOLERS22 program, a project of the Solar-Terrestrial Energy Program (STEP), has posed two questions to define its work: What are the daily flux values of the solar spectral irradiance in the X ray, EUV, UV, visible and infrared wavelength ranges and the total solar irradiance? and What evolving solar spatial structures cause the temporal variations of these full-disk fluxes? One project objective is to develop improved solar flux models for the irradiance variations.

In general, this period of proxy correlation concluded with important advances. A common strength of all six models is that each uses multiple indices to estimate solar EUV emissions whose source regions are in different temperature layers of the solar atmosphere. Each model represents, to first order, the 27-day (solar rotation), intermediate-term (active region evolution and decay), and long-term 11-year (solar cycle) relative variability of the ir-

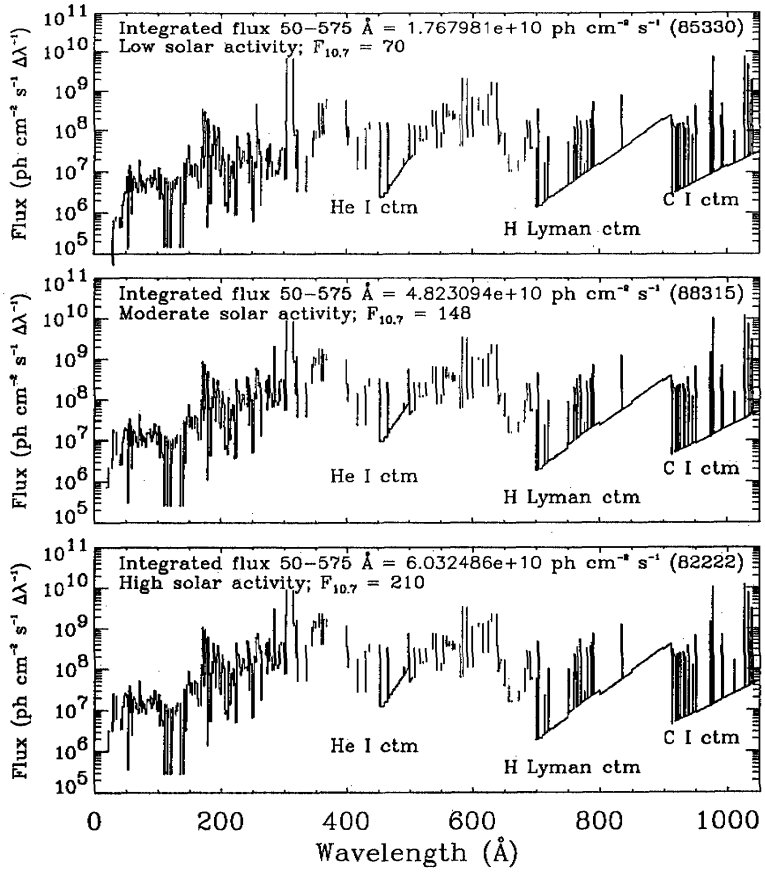

Fig. 8. The EUV91 model solar EUV spectrum for November 26, 1985 (low solar activity), for November 10, 1988 (moderate activity), and for August 10, 1982 (high activity) are shown in three panels. The total integrated flux for 5 to 57.5 nm is 17.7×10^9 ph cm^{-2} s^{-1} for the November 1985 case, 48.2×10^9 ph cm^{-2} s^{-1} for the November 1988 case, and 60.3×10^9 ph cm^{-2} s^{-1} for the August 1982 case. The He I continuum is visible between 45 and 50.4 nm, the H Lyman continuum is between 70 and 91.2 nm, and the C I continuum is between 91.3 and 105 nm in each panel. Discrete emission lines rise considerably higher than the continua. The modeled spectrum is based on the wavelength ranges of the SC#21REFW spectrum and contains missing lines.

radiance. Each model also estimates the magnitude, phase, rise, and decline of the measured EUV emissions with uncertainty (compared to the data and neglecting the uncertainty of the data) from less than ± 10% to greater than a factor of ± 2 depending upon wavelength and model. Several generally reliable ground- and space-based proxies have been found for the chromospheric and coronal emissions that are now in use or are being developed for use in models. Lyman-α and He I 1083-nm EW emissions were found to be good full-disk indices for chromospheric emissions and $F_{10.7}$ daily and 81-day mean values were found to be acceptable indices for transition region and coronal emissions.

Current EUV models are specifically designed for use by the aeronomy community to provide thermospheric energy inputs. The solar models provide irradiances at a variety of spectral resolutions for campaign dates, solar maximum to minimum periods, and terrestrial seasonal time frames. On the basis of the models and data available at the end of the 1980s, *Lean* [1988] and *Tobiska* [1988] graphically show spectral irradiance ratios for solar maximum to minimum by wavelength and show unit optical depth penetration into the terrestrial atmosphere for the EUV wavelengths during solar maximum and minimum conditions.

There are a number of weaknesses still remaining in the models. First, each of the models has inconsistencies, often in absolute magnitude of emission, between modeled flux values and observed data. In large part, these inconsistencies can be traced to phase and amplitude differences in temporal variation between proxies and data; they can also be traced to errors of approximation which are inherent in linear or nonlinear regression techniques as applied to the proxy-data correlations. Additionally, sparse or discontinuous EUV data also contribute to model uncertainty. These missing data combine with flux magnitude disagreements between the independent EUV data sets that are used in model correlations. Weighting some data sets over others further magnifies modeling uncertainties.

A second weakness is that two of the models (SERF1 and Nusinov) rely solely on one data set (AE-E) for temporal variation and for all flux absolute magnitudes. The other models are heavily influenced by the AE-E data set for temporal variation and rely on one rocket measurement for absolute magnitudes below 15 nm at any spectral resolution.

A third weakness is that limited comparison between the solar EUV models and their inputs into thermospheric/ionospheric

TABLE 1. EUV91 Modeled Irradiances for November 10, 1988

λ*	Φ†	λ	Φ	λ	Φ	λ	Φ	λ	Φ
18.62	7.22E+05	67.14	9.22E+06	90.14	9.53E+06	127.65	1.18E+07	193.52	1.84E+08
18.97	7.22E+05	67.35	6.15E+06	90.45	6.15E+06	129.87	8.88E+06	195.13	3.01E+08
21.6	2.16E+06	68.35	7.07E+06	90.71	9.22E+06	130.3	2.61E+05	196.52	2.73E+07
21.8	7.22E+05	69.65	4.24E+07	91	1.20E+07	131.02	1.36E+07	196.65	8.17E+06
22.1	2.16E+06	70	3.07E+05	91.48	5.84E+06	131.21	1.25E+07	197.44	1.13E+07
28.47	3.61E+06	70.54	1.01E+07	91.69	1.66E+07	136.21	2.61E+05	198.58	2.00E+07
28.79	1.80E+07	70.75	9.22E+06	91.81	1.48E+07	136.28	2.61E+05	200.02	6.32E+07
29.52	1.59E+07	71	1.35E+07	92.09	1.17E+07	136.34	2.61E+05	201.13	1.07E+08
30.02	3.88E+06	71.94	3.69E+06	92.81	1.17E+07	136.45	2.61E+05	202.05	1.66E+08
30.43	2.59E+06	72.31	1.97E+07	93.61	1.72E+07	136.48	2.61E+05	202.64	9.31E+07
33.74	4.74E+06	72.63	4.92E+06	94.07	2.52E+07	141.2	2.95E+07	203.81	8.22E+07
40.95	2.59E+06	72.8	6.46E+06	94.25	3.07E+05	144.27	2.87E+06	204.25	3.03E+07
43.76	9.06E+06	72.95	1.05E+07	94.39	5.23E+06	145.04	3.68E+07	204.94	2.06E+07
44.02	3.45E+06	73.47	1.54E+06	94.9	3.07E+05	148.4	7.68E+07	206.26	6.32E+06
44.16	3.88E+06	73.55	5.84E+06	95.37	1.48E+07	150.1	2.14E+07	206.38	6.32E+06
45.66	2.16E+06	74.21	7.69E+06	95.51	8.92E+06	152.15	3.69E+07	207.46	6.32E+06
46.4	1.16E+07	74.44	4.00E+06	95.81	8.92E+06	154.18	1.94E+07	208.33	7.58E+06
46.67	1.73E+07	74.83	1.23E+07	96.05	2.52E+07	157.73	1.75E+07	209.63	3.79E+06
47.87	1.94E+07	75.03	1.41E+07	96.49	5.84E+06	158.37	4.00E+07	209.78	4.63E+06
49.22	1.85E+07	75.29	7.69E+06	96.83	8.30E+06	159.98	3.66E+07	211.32	1.15E+08
50.52	1.72E+07	75.46	1.17E+07	97.12	1.60E+07	160.37	3.10E+07	212.14	3.37E+07
50.69	1.72E+07	75.73	7.69E+06	97.51	9.22E+06	162	1.55E+07	213.78	1.05E+07
52.3	1.08E+07	76.01	9.84E+06	97.87	7.07E+06	164.15	1.04E+07	214.75	1.81E+07
52.91	3.07E+05	76.48	3.07E+06	98.12	8.30E+06	167.5	5.49E+07	215.16	6.11E+07
54.15	2.52E+07	76.83	1.26E+07	98.26	8.30E+06	168.17	1.01E+08	216.88	4.21E+07
54.42	1.11E+07	76.94	1.01E+07	98.5	7.99E+06	168.55	5.77E+07	218.19	7.79E+07
55.06	1.23E+07	77.3	8.92E+06	99.71	6.15E+06	168.92	3.55E+07	219.13	3.03E+07
55.34	3.26E+07	77.74	1.20E+07	99.99	8.30E+06	169.7	6.59E+07	220.08	4.34E+07
56.08	7.38E+06	78.56	9.22E+06	100.54	2.19E+07	171.08	8.66E+08	221.44	7.50E+07
56.92	2.28E+07	78.7	8.61E+06	103.01	3.92E+06	172.17	3.15E+07	221.82	3.79E+06
57.36	1.91E+07	79.08	5.84E+06	103.15	2.61E+05	173.08	6.03E+07	224.74	1.76E+08
57.56	1.54E+07	79.48	5.53E+06	103.58	1.59E+07	174.58	7.57E+08	225.12	3.22E+08
57.88	1.32E+07	79.76	7.07E+06	103.94	1.59E+07	175.26	9.32E+07	227.01	1.75E+08
58.96	2.15E+06	80	4.30E+06	105.23	1.33E+07	177.24	4.58E+08	227.19	8.43E+05
59.62	2.15E+06	80.55	7.07E+06	106.25	5.22E+06	178.05	5.77E+07	227.47	1.24E+08
60.3	7.69E+06	82.43	1.51E+07	108.05	3.92E+06	179.27	1.13E+06	228.7	8.59E+07
60.85	1.11E+07	82.74	7.99E+06	109.98	2.61E+05	179.75	5.80E+07	230.65	5.48E+07
61.07	1.78E+07	82.84	7.99E+06	110.56	2.61E+05	180.41	5.04E+08	231.55	6.66E+07
61.63	8.92E+06	83.42	1.38E+07	110.62	2.61E+05	181.14	5.97E+07	232.6	9.69E+07
61.9	1.54E+07	83.67	1.17E+07	110.76	3.92E+06	182.17	6.51E+07	233.84	1.52E+07
62.3	3.07E+05	84	1.57E+07	111.16	2.61E+05	183.45	4.22E+06	234.38	1.39E+08
62.35	3.38E+06	86.77	1.41E+07	111.25	1.25E+07	184.53	1.23E+08	237.12	1.64E+07
62.77	1.05E+07	86.86	5.84E+06	113.8	7.84E+06	184.8	6.48E+06	237.2	8.43E+05
63.16	1.01E+07	86.98	9.53E+06	114.09	6.79E+06	185.21	5.13E+07	237.33	8.13E+07
63.3	1.66E+07	87.3	7.38E+06	114.24	2.61E+05	186.6	9.01E+06	239.87	8.43E+07
63.65	1.26E+07	87.61	6.15E+06	115.39	2.61E+05	186.87	6.51E+07	240.71	7.04E+07
64.11	3.38E+06	88.09	1.38E+07	115.82	6.27E+06	187.95	1.97E+06	241.74	3.77E+08
64.6	7.69E+06	88.11	1.88E+07	116.75	1.02E+07	188.23	2.73E+07	243.03	3.67E+08
65.21	9.22E+06	88.14	3.07E+05	117.2	6.79E+06	188.31	3.38E+08	243.78	2.40E+07
65.71	1.26E+07	88.42	5.84E+06	120.4	2.61E+05	190.02	1.19E+08	244.92	2.44E+08
65.85	9.22E+06	88.64	7.38E+06	121.15	2.61E+05	191.04	2.96E+07	245.94	4.21E+06
66.26	9.22E+05	88.9	1.17E+07	121.79	2.87E+06	191.34	2.53E+07	246.21	9.61E+07
66.3	1.17E+07	89.14	8.30E+06	122.7	1.07E+07	192.4	1.13E+08	246.91	4.93E+07
66.37	1.23E+06	89.7	9.22E+06	123.5	6.79E+06	192.82	1.66E+08	247.18	1.05E+08

models has been done. This is in spite of the fact that there is widespread aeronomy community use of the solar minimum and solar maximum reference spectra that were derived from the AE-E data set [e.g., *Roble, 1987*; *Donnelly, 1987a*]. Donnelly (private communication, 1990) noted that SERF1 and SERF2 concentrated on relative temporal variations rather than absolute fluxes and that no comparisons with spatially resolved solar measurements had yet been made. In addition, no terrestrial atmosphere model evaluations using these temporal solar flux models had been completed by the end of the decade.

Buonsanto et al. [1992] have begun this process of comparing atmospheric data sets and solar EUV models and have obtained interesting results. They compared measured and modeled electron densities in the E-F_1 region ionosphere. The modeled electron densities were produced by two separate photochemical models using SERF1, EUV91, and rocket-measured solar EUV flux. They concluded that although the photochemical models generally underestimated the atmospheric data, especially in winter, the model results were an improvement over previous work when the new solar data were used. In particular, since the EUV91 model pro-